

Antibacterial and photoluminescence activity of TiO₂/ZnO nanocomposite

*E.Nirmala Devi, #T.Subba Rao

*Department of Physics, Rayalaseema University, Kurnool, AP, India.

#Dept of Physics ,S.K.University Ananthapuram, AP, India.

Abstract - Nano-composite of titania and zinc oxide was synthesized by sol-gel method and characterized by XRD, FTIR, DLS, FE-SEM, HR-TEM and PL. With an average crystallite size of 26 nm, the structural analysis from XRD reveals the arrangement TiO₂/ZnO nanocomposite. The antibacterial activity of the synthesized nanocomposite was measured with the help of well diffusion plate method and disclosed finest antibacterial performance was monitored. The effects were specified a greater competence on antibacterial properties against on both gram positive and gram negative effects of nanocomposite. The TiO₂ was used to augment the photo-catalytic activity while ZnO was used to eradicate detrimental bacteria.

Key words: sol-gel method, TiO₂/ZnO nanocomposite, characterization, antibacterial and photoluminescence.

I. INTRODUCTION

The nanotechnology and nanoscience are making use of nanomaterials in several fields to articulate the significance of the nanomaterials. Based on the attributes, particularly the band gap of semiconductors is chiefly rely on the particle size [1]. Metal oxide semiconductors (ZnO, TiO₂, CuO, SnO₂ etc) have copious appliances[2]. Properties of nanocomposites augmented with greater thrust as they posses captivating optical, catalytic, magnetic and mechanical properties, used as photo catalysts [3-7]. ZnO is a direct band gap semiconductor (3.37 eV) that displays elevated optical transparency and luminescent properties in the near UV [8]. The gigantic exciton B.E(60 meV) would allow excitonic changeovers still at room temperature. Because of the novel properties like low cost, thermal conductivity high refractive index, antibacterial and UV protection it could be used in myriad applications[9] such as UV light producing appliances[10-11] ethanol gas sensor[12], photo catalysts with sophisticated oxidation features[13], varistors[14] sunscreens and facial creams[15]. TiO₂ is not a direct semiconductor (3.18eV) and because of its positive properties such as innocuous, comparatively inexpensive and chemically constancy, incredible applications in diverse fields such as paints [16]. Photo catalytic is an outstanding property that has been widely used in environmental pollutant elimination [17] UV protection agents (sunscreens)[18] photovoltaic [19] sensing [20] toothpaste[21], electronic devices[22], high efficiency solar cell[23], hydrogen generation[24] Photo chromic devices, super capacitors[25-27] and additionally it is made use in optical and defensive appliances because of its lofty transparency in the visible area, radiant mechanical duality and chemical constancy in aqueous solution, membranes in the cells of solar. The death of cell by TiO₂ photo catalyst

is specified to the mixture of cell membrane damage and oxidation assault of internal cellular components [28-29]. Based on the equivalent band gap structure, among the semiconductors, ZnO and TiO₂ display good photo catalytic characteristic due to its wide band gap and photo generated e-hole duo. The proficiency of photo catalyst can be augmented with these nanocomposites. Environment, water, health are damaged by chemical pollution like heavy metals, solvents dyes and pesticides. Adsorption and photo catalytic degradation are used as effective method to remove toxic heavy metal ions and organic pollutants from waste water. Advanced oxidation process (AOPs) produces hydroxyl radicals.(HO⁻)used to degrade toxic organic pollutants waste into non-toxic by products. Heterogeneous photo catalysis does engage the consumption of semiconductor catalyst (ZnO and TiO₂) irradiated with light used to generate extremely reactive transitory species(OH⁻, O₂, H₂O₂). These species able to react practically with all classes of organic compounds, resulting in complete good compound that is formation of CO₂, water and inorganic salts. Antibacterial activity of the nanoparticles relied on structure, atypical properties, change and types of micro-organisms. Owing to oxidation stress, the cell membrane of the bacteria can be damaged by using these nanocomposites. In recent times, the inorganic nanocomposites' use does act as antibacterial agents because of the production of reactive of oxygen species (ROS) on the outer layer of these oxides. These inorganic antibacterial drug agents are more secure and constant than organic antimicrobial agents. In the midst of innumerable techniques, ZnO/TiO₂ nanocomposites are synthesized by sol-gel method. The nanocomposites are prepared at economical price, low temperature, chemical solidity and eco-friendly nature.

II. DETAILS OF EXPERIMENTATION

$$D = \frac{k\lambda}{\beta \cos\theta}$$

2.1 Synthesis method

Zinc acetate dehydrate (5.48 gm) was liquefied in 50ml of deionized water and concurrently 8.5 ml of titanium isopropoxide was dissolved in 50ml of ethanol solution and stirred for 1 hour to attain a translucent solution and subsequently arranged a solution of NaOH (2M). The NaOH solution was added drop by drop and stirred robustly to reach pH above 10. The attained milk white solution was heated at 90 °C for 40 min. The milky solution was centrifuged at 3000 rpm for 15 min and attained precipitates were washed with methanol and repeated the analogous process 5 times to remove the unnecessary compounds entirely. The solution made dry at 100 °C for sixteen hours in an oven and later calcinated at 400 °C for two hours in muffle furnace.

2.2 Evaluation of bacterial activity

Antimicrobial activities of TiO₂/ZnO nanocomposites were evaluated using well diffusion method on Muller-Hinton Agar (MHA). The reserve zones were described in millimetre (mm). S.aureus and E.Coil (Gram positive and Gram Negative) were used for the antibacterial activity. The MHA agar plate were inoculated with bacterial strain under aseptic situations and well (3mm diameters) were crammed with a variety of concentrations of the test compound and incubated at 37°C for 24 h. After the stage of incubation, the diameter of the growth inhibition zones were calculated. The well's intensity is amplified with the improved solution's concentration.

III. RESULTS AND DISCUSSION

3.1 XRD Analysis

X-ray diffraction analysis studied the phase composition and the structure. Fig 1 projects XRD outline of organized TiO₂/ZnO nanocomposite. From the XRD pattern and corresponding characteristic 2θ of diffraction peaks, it can be substantiated that ZnO nps in the given sample are identified as hexagonal zincite phase for the sharp diffraction peaks located at 2θ = 31.8°, 34.6°, 36.2°, 48.56°, 52°, 62.8° and 67.8° are allocated to the crystal planes (100), (002), (101), (102), (110), (103) and (112) correspondingly. All these diffraction peaks are matched with standard spectrum (JCPDS card No.36-1451). Besides, strong peaks are observed at 2θ position 25.24°, 36.3°, 62, 67.8° are assigned to the crystal planes (110), (101), (310), (301) indicates the formation of anatase phase in TiO₂ structure in nanocomposites (JCPDS card No.89-6975). The intensities of the main peaks of ZnO and TiO₂ in case of composite as different stages and no other stages are monitored in this analysis of XRD. The sharp diffraction peak is observed at (101) crystal plane has both phases (ZnO and TiO₂). [30-31]. The nanocomposite's crystallite size was measured by using scherrer formula

Where the crystallite size (nm) is indicated by D, the x-ray wavelength is by λ (CuKα radiation and equal to 0.154nm), the Bragg diffraction angle is by Θ, and β is the full width half maximum (FWHM) of the XRD peak coming into view at the diffraction angle. The average crystalline size was calculated it was found to be about 26nm. [31-32].

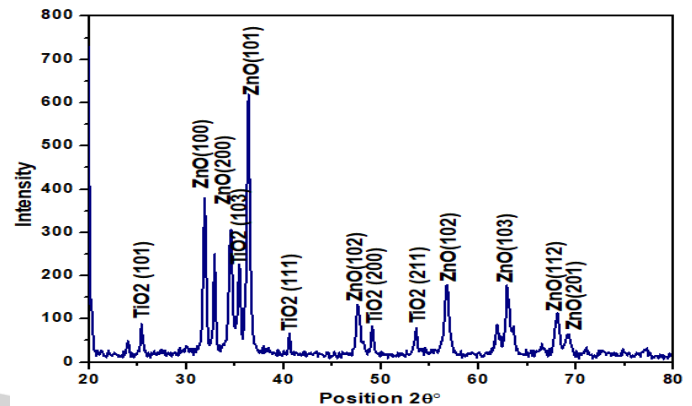


Fig. 1. XRD Diffraction pattern of ZnO/TiO₂ nanocomposites

3.2 FT-IR analysis :

Fig (2) shows the spectrum of equipped composite in the range of 500-4000 cm⁻¹. The finger prints are extremely intricate and cannot guessed exact range for equipped nanocomposite. The shorter assimilation peaks from 400-700 cm⁻¹ corresponds to Zn-O bond and Ti-O-Ti bond. The band between 800-900 cm⁻¹ is assigned to the Zn-O-Ti stretching mode in the nanocomposites. The absorption band around 1100 cm⁻¹ is described to carboxylic acid (C=O). The absorption band from 1300 -1400 cm⁻¹ is associated with vibration modes of Ti-O and Ti-OH in the given nanocomposite. The peak at 1430 cm⁻¹ is because of the symmetric expanding of carboxyl group. The sharp peak at 1510 cm⁻¹ is because of asymmetric expanding of carboxyl group. The band at 1600 cm⁻¹ is allotted to H-O-H bending vibration mode owing to the assimilation of moisture. The peak at 2800 cm⁻¹ corresponds to C-H expanding bond. The smaller band at 3500 cm⁻¹ which can be allotted to the expanding vibration bond of hydroxyl groups (O-H). [32-33].

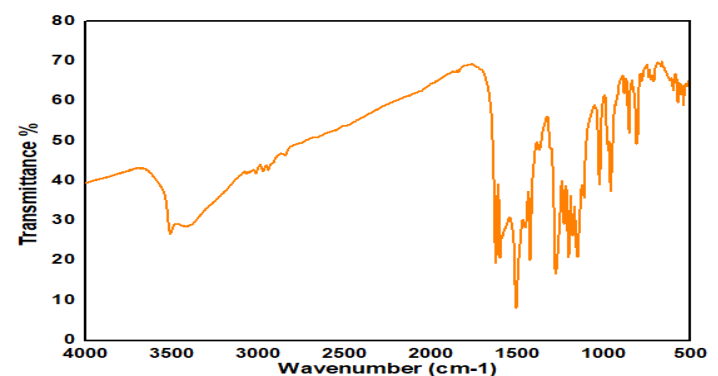


Fig. 2. FT IR Spectrum of TiO₂/ZnO nanocomposites

3.3 FE-SEM Analysis:

Field electronics Scanning Electron microscopy was employed for the surface morphology. From Fig 3(a) it is complex to percept the particle size clearly and display grainy size surface morphology from FE-SEM. The morphology comprises of spherical particles are disseminated homogeneously equal in size and also agglomerated in Fig.3(c)

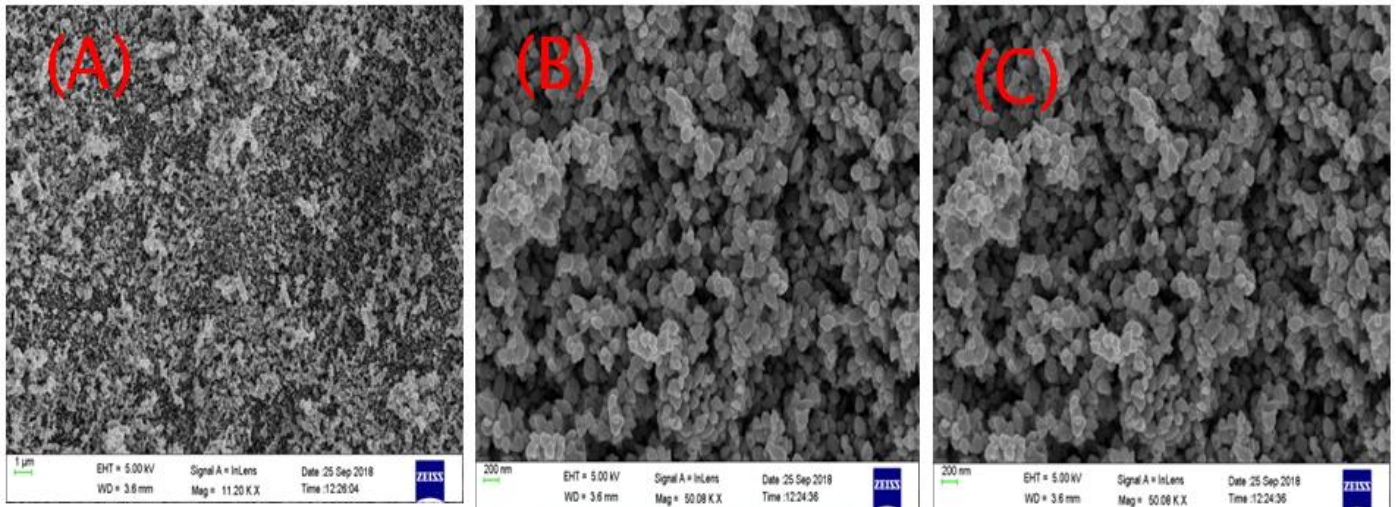


Fig.3.(a), (b) and (c) SEM images of ZnO/TiO₂ nanocomposites

3.4 HR-TEM analysis

Fig 4(a) and 4(b) show the images of HR-.TEM of TiO₂/ZnO nanocomposites. HR-SEM were used to provide the particles distribution and to guess the size of the particles, which was then compared with the crystalline size obtained from XRD. The images made known that the co-existence of ZnO and TiO₂ particles in the nanocomposite and that were observed at different magnifications. It has been visualized that the shape of the particles are spherical structure and distributed evenly. The average size of the particles is about 10 to 20 nm .respectively

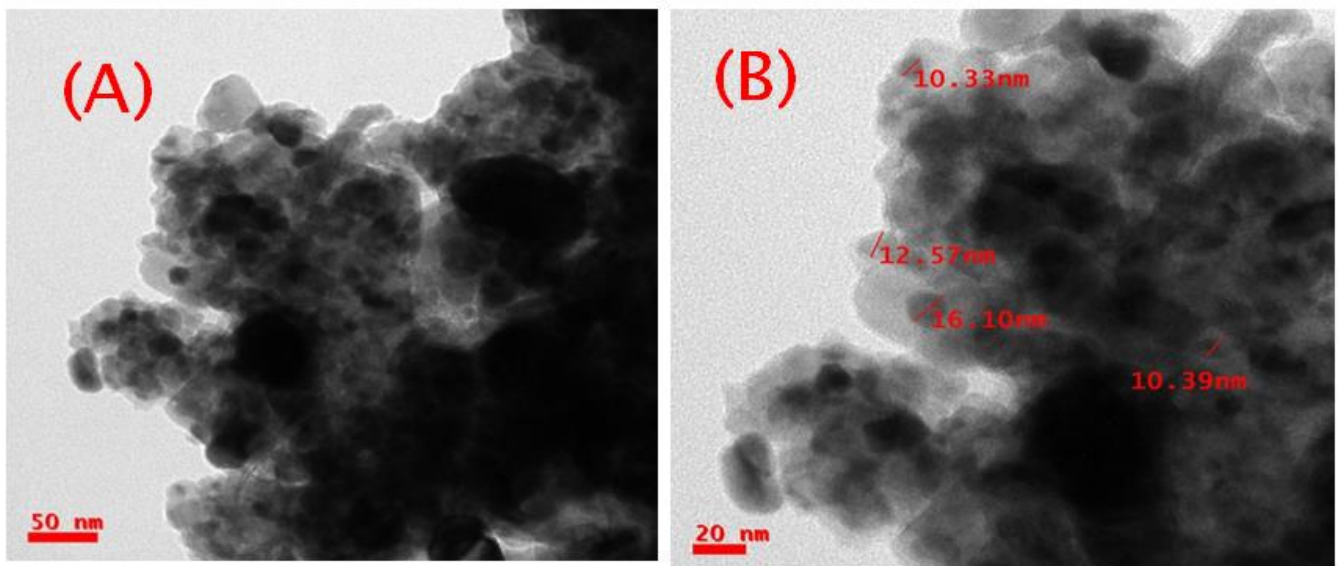


Fig.4. (a) and (b) HR-TEM images of TiO₂/ZnO nanocomposites

3.5 Particle Analysis:

The average particle shape was calculated by particle shape analyser with the help of DLS principle .The prepare TiO₂/ZnO nanocomposites were dispensed in ethanol solution. The particles are in Brownian motion in the given solution. The YD- laser light was intensed on this solution is placed in particle size analyser. The light is scattered from no. of different sizes. The histogram curve is observed between frequency (%) and diameter (nm) .The average value of the disseminated histogram was taken as average particle shape of the proper nanocomposites. The obtained average particles size for TiO₂/ZnO is 82.7 nm. The mean size of the nanocomposites ranged from 10 to 100nm.

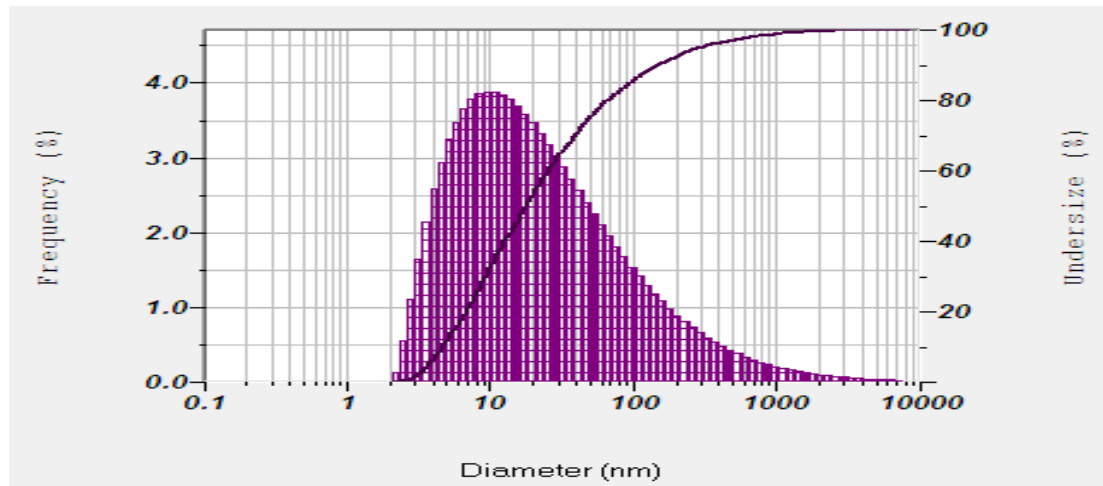


Fig.5. DLS analysis of ZnO/TiO₂ nanocomposites

IV. ANTIBACTERIAL ACTIVITY

Antibacterial activity was assessed against with two bacterial strains namely E.Coli, S.aureus .This bacterial strains were inoculated in MH medium with various concentrations of(50µl,100µl,150µl,200 µl)semiconductor oxides of TiO₂/ZnO nanocomposites. This sample of bacteria was incubated at 37°C for 24 hr. Typically, these semiconductor exhibits good antibacterial, photocatalyst and self-cleaning properties. Due to this Photo catalyst properties, the ZnO and TiO₂ nps generates e- hole pair process. The procedure results in the generation of ROS. The produced ROS contains hydroxyl radicals and peroxides groups. These groups react with structure of cellular components such as DNA and cellular enzymes and conclude to kill the microorganism cell.

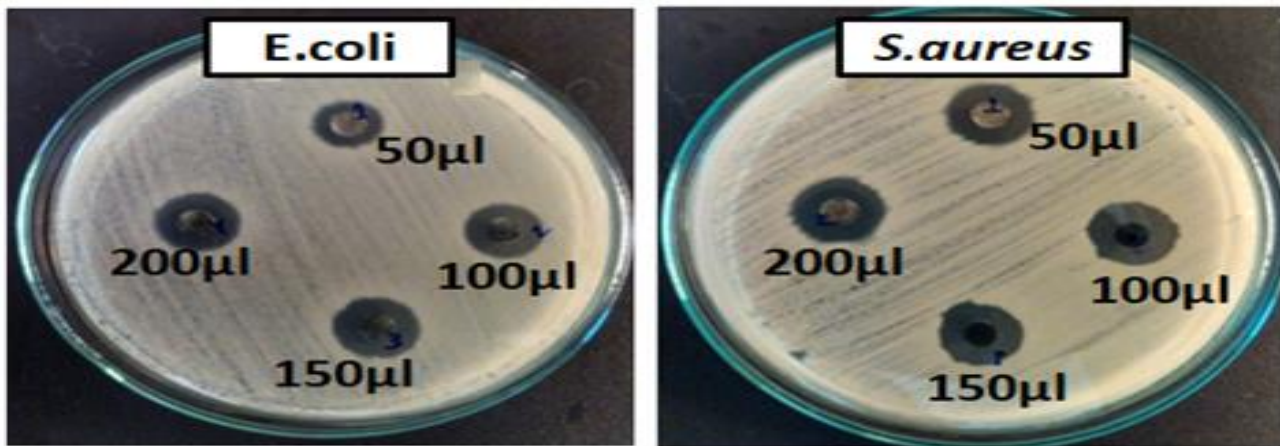


Fig.6. Effect of ZnO/TiO₂ nanocomposites on gram positive (S.aureus) and gram negative (E.Coli).

Table.1 Antibacterial activity of TiO₂/ZnO:

S. No.	Compounds	Zone of inhibition (Diameter in mm at stock conc. 1mg/mL)							
		NPs							
		<i>Escherichia coli</i> (-ve)				<i>Staphylococcus aureus</i> (+ve)			
		50 µl	100 µl	150 µl	200 µl	50 µl	100 µl	150 µl	200 µl
1.	ZnO-TiO ₂	10 ± 0.13	14 ± 0.25	15 ± 0.52	17 ± 0.61	11 ± 0.19	14 ± 0.32	18 ± 0.67	20 ± 0.89

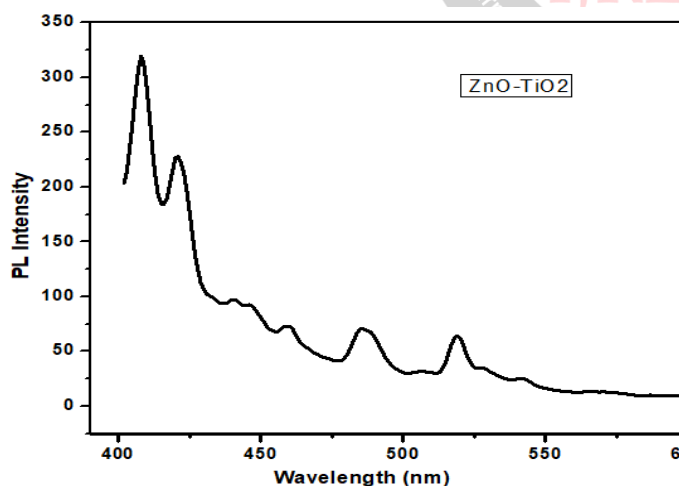
Photoluminescence Spectroscopy of TiO₂/ZnO nanocomposites:

PL spectroscopy is a potential instrument used to study the imperfections in its structure and energy bands in the materials. Luminescence characteristics as well rely on remaining vital features which comprises solvent,

atmosphere, starting materials etc and is attributed to different processing conditions during synthesis process [36].

At room temperature,the PL studies of the TiO₂/ZnO nanocomposite were excuted. In the fig the PL spectra of TiO₂/ZnO nanocomposite displayed five emanation peaks

408nm,420nm ,460nm,485nm and 520nm with an excitation wavelength of 380nm. In this spectra, near band gap and blue or deep level emission peaks are observed. The NBE's of nanocomposite at 420nm corresponds to the direct band gaps of the oxides. owing to crystal defects the corresponding DLE at 485nm are propable. These flaws presumably happens because the vacancies of oxygen in the lattice [37]. Formation of hetero junction slows down the electron-hole recombination and as a result decreases the production. It is pertinent to affirm that the valence and conduction bands refer to the oxidized and reduced states in the semiconductor. The reduced form of Ti^{4+} or Zn^{2+} (i.e., Ti^{3+} or Zn^+) is referred by the conduction band(CB)electrons and the valence band (VB) hole corresponds to the oxidized form of O_2 (i.e., O_2^-). The excitation of the band gap is the photoexcitation of an electron from O_2^- to Ti^{4+} or Zn^{2+} and the recombination of electron-hole is reversion of the electron from Ti^{3+} or Zn^+ to. It is appealing to state that any emanation near 432 nm is not shown by the PL spectrum of the composite which corresponds to the indirect band gap attained from the Tauc plot. In indirect band gap changeover, electron from the CB recombines with hole in the VB not directly through traps devoid emission of photon. One more prominent trait of the PL spectrum of TiO_2/ZnO is that it exhibit strong blue emission at 461 nm. This is feasible due to the recombination of electron in singly occupied oxygen vacancy with the photogenerated hole in the VB of deposited ZnO [38]. It also displays abroad green emission band with max around 520nm which most likely comes from the TiO_2 with anatase structure. A green luminescence band is monitored due to radiative recombination self trapped excitations.



V. CONCLUSION

Sol-gel method has fruitfully synthesized TiO_2/ZnO nanocomposites. The synthesized nanocomposites were used and tested for their antibacterial and photo catalyst properties. Because of photo catalyst features, nanocomposites disclosed the fine antimicrobial activity on both gram positive and gram negative bacteria. The XRD

pattern illustrated different crystalline phases such as ZnO (wurtzite hexagonal) and TiO_2 (anatase). The average crystalline particle were measured by Debye-Scherrer's formula and also from particle analyser. The FE-SEM results displayed the formation of spherical shaped and also distributed uniformly of ZnO/TiO_2 nanocomposites. The HR-SEM outcomes projected the precise size and shape and arrangement of the nanocomposites. The intensity of PL is increased is due to oxygen vacancy defect trapping charge carriers while reducing the e^- -hole recombination in the nanocomposites.

ACKNOWLEDGMENTS

I would like to convey my gratitude and heartfelt thanks to the Department of Physics, Rayalaseema University for allowing me to use the laboratory for my research. I am indebted to them for their esteemed cooperation.

REFERENCES

- [1]. U.Hameed, Kabeer A. Khan, Ullah Khan, "ZnO/TiO2 Nanocomposite Synthesized by Sol Gel from Highly Soluble Single Source Molecular Precursor" J.Chinese physical Society. 27(2014), 548-554.
- [2]. A.Stoyanova, H.Hitkova, Synthesis and Antibacterial Activity of TiO_2/ZnO Nanocomposites prepared via NonHydrolytic Route. J.Chemical Technology and Metallurgy. 48(2013), 154-161.
- [3]. A. A. Farghali, M. Moussa, M. H. Khedr, Synthesis and characterization of novel conductive and magnetic nanocomposites, J. Alloys Compd. 499 (2010) 98-103.
- [4]. N. M. Deraz, Size and crystallinity-dependent magnetic properties of copper ferrite nano-particles, J. Alloys Compd. 501 (2010) 317-325.
- [5]. L. D. Zhao, B. P. Zhang, J. F. Li, M. Zhou, W.S. Liu, J. Liu, Thermoelectric and mechanical properties of nano-SiC-dispersed Bi_2Te_3 fabricated by mechanical alloying and spark plasma sintering, J. Alloys Compd. 455 (2008) 259-264.
- [6]. P.G. Li, M. Lei, W.H. Tang, X. Guo, X. Wang, Facile route to straight SnO_2 nanowires and their optical properties, J. Alloys Compd. 477 (2009) 515-518.
- [7]. X. Hou, S. Zhou, Y. Li, W. Li, Luminescent properties of nanosized $Y_2O_3: Eu$ fabricated by co-precipitation method, J. Alloys Compd. 494 (2010) 382-385.
- [8]. Wenfeng Shen, Yan Zhao, T. Caibei Zhang, The preparation of ZnO based gas-sensing thin films by ink-jet printing method, J. Thin Solid Films. 483 (2010) 382 - 387
- [9]. Riyadh M. Alwan, Quraish A, et.al, Synthesis of Zinc Oxide Nanoparticles via Sol - Gel Route and Their Characterization, J. Nanoscience and Nanotechnology 5(1)(2015) 1-6.
- [10]. N. Izu, K. Shimada, T. Akamatsu, T. Itoh, W. Shin, K. Shiraishi, T. Usui, Polyol synthesis of Al-doped ZnO spherical nanoparticles and their UV-vis-NIR absorption properties, Ceram. Int. 40 (2014) 8775-8781.
- [11]. M. Rajalakshmi, S. Sohila, S. Ramya, R. Divakar, C. Ghosh, S. Kalavathi, Blue

green and UV emitting ZnO nanoparticles synthesized through a non-aqueous route, *Opt. Mater.* 34 (2012) 1241–1245.

[12]. R.-C. Xie, J. Shang, Morphological control in solvothermal synthesis of titanium oxide, *J. Mater. Sci.* 42 (2007) 6583–6589.

[13]. K. Mageshwari, D. Nataraj, T. Pal, R. Sathyamoorthy, J. Park, Improved photocatalytic activity of ZnO coupled CuO nanocomposites synthesized by reflux condensation method, *J. Alloys Compd.* 625 (2015) 362–370.

[14]. A.B. Corradi, F. Bondioli, et al. Grippo, E. Mariani, C. Villa, Conventional and microwave-hydrothermal synthesis of TiO₂ nanopowders, *J. Am. Ceram. Soc.* 88 (2005) 2639–2641.

[15]. S. Komarneni, D. Noh Young, et al. Solvothermal/hydrothermal synthesis of metal oxides and metal powders with and without microwaves, *Z. Naturforsch. B* (2010) 1033.

[16]. Bari, A. R., Shinde, M. D., Vinita. D. & Patil, L. A. Synthesis of 1D, 2D and 3D ZnO Polycrystalline Nanostructures Using Sol-Gel Method. *Journal of Nanotechnology*, 6 (2009) 1–8.

[17]. Wahab, H.A & Salama, A.A et al. (2013). Optical, structural and morphological studies of ZnO nano-rod thin film using sol-gel. 3, 46-51. 4. Chai, C. (2012).

[18]. V. Chhabra, V. Pillai, B.K. Mishra, A. Morrone, D.O. Shah, Synthesis, characterization, and properties of micro emulsion-mediated nanophase TiO₂ particles, *Langmuir* 11 (1995) 3307–3311.

[19]. J. Eastoe, B. Warne, Nanoparticle and polymer synthesis in micro emulsions, *Curr. Opin. Colloid Interface Sci.* 1 (1996) 800–805.

[20]. Yung, K., Ming, H., Yen, C. & Chao The Global Market for Zinc Oxide Nanopowders 2012. New Report on Global Zinc Oxide Nanopowder Market, H.5 (2012) 134–140

[21]. M. Andersson, L. Österlund, S. Ljungström, A. Palmqvist, Preparation of nanosize anatase and rutile TiO₂ by hydrothermal treatment of microemulsions and their activity for photocatalytic wet oxidation of phenol, *J. Phys. Chem. B* 106 (2002) 10674–10679.

[22]. U. Bach, D. Corr, Nanomaterials-Based Electrochromics for Paper- Quality Displays, *Adv. Mater. B* 14(2002)845–848

[23]. A. Dhara, B. Show, A. Baral, S. Chabri, A. Sinha, N. R. Bandopadhyay, N. Mukherjee, Core-shell CuO-ZnO p-n heterojunction with high specific area for enhanced photoelectrochemical (PEC) energy conversion, *Solar Energy* 1369 (2016) 327–332

[24]. A. Kargar, Y. Jing, S.J. Kim, C.T. Riley, X. Pan, D. Wang, ZnO/CuO heterojunction branched nanowires for photoelectrochemical hydrogen generation, *ACS Nano* 7 (2013) 16999–17007.

[25]. B. Pal, B.L. Vijayan, S.G. Krishnan, M. Harilal, W.J. Basirun, A. Lowe, M.M. Yusoff, R. Jose, Hydrothermal syntheses of tungsten doped TiO₂ and TiO₂/WO₃ composite using metal oxide precursors for charge storage applications, *J. Alloys compd.* 740 (2018) 703–710.

[26]. M. Harilal, S.G. Krishnan, A. Yar, I.I. Misnon, M. V. Reddy, M. M. Yusoff, J.O. Dennis, R. Jose, Pseudocapacitive Charge Storage in Single-Step-Synthesized CoO–MnO₂–MnCo₂O₄ Hybrid Nanowires in Aqueous Alkaline Electrolytes, *J. Phys.*

Chem. C 121(2017) 21171–21183.

[27]. M. Harilal, S.G. Krishnan, B.L. Vijayan, M.V. Reddy, S. Adams, A. R. Barron, M. M. Yusoff, R. Jose, Continuous nanobelts of nickel oxide–cobalt oxide hybrid with improved capacitive charge storage properties, *Mat. Design* 122 (2017) 376–384.

[28]. A. G. Rincon, C. Pulgarin, N. Adler, P. Peringer, Interaction between *E. coli* inactivation and DBP-precursors-dihydroxybenzene isomers in the photocatalytic process of drinking-water disinfection with TiO₂, *J Photochem Photobiol A: Chem.* 139 (2001) 233–241.

[29]. K. Sunada, T. Watanabe, K. Hashimoto, Studies on photokilling of bacteria on TiO₂ thin film, *J Photochem Photobiol A: Chem.* 156(2003)227–233.

[30]. Liqin Wang, Xiujun Fu Yang Han, et al. Preparation, Characterization, and Photocatalytic Activity of TiO₂/ZnO Nanocomposites. *J. Nanomaterials*, Article 1D321459(2013), 1–6.

[31]. S.A. Siuleiman, D.V. Raichev, Nanosized composite ZnO/TiO₂ thin films for photocatalytic applications. *J. Bulgarian chemical communications*, Vol 45(2013), 649–654.

[32]. K.S. Babu, V. Narayanan, Hydrothermal synthesis of hydrated zinc oxide nanoparticles and its Characterization, *Chem. Sci. Trans.* 2(S1) (2013) S33–S36.

[33]. Mitra Gholamia, Mehdi Shirzad-Sibonia, Synthesis, characterization, and application of ZnO/TiO₂ nanocomposite for photocatalysis of a herbicide (Bentazon) *J. Desalination and Water Treatment* (2015) 1–13

[34]. Jaskaran Singh Malhotra, Arnav Sharma Investigations on Photocatalytic, Antimicrobial and Magnetic Properties of Sol-Gel-Synthesized Ga-Doped ZnO Nanoparticles. *J. Nanoscience*. Vol. 17(2018), 1850014–24

[35]. Yu Hang Leung, Xiaoying Xu, Toxicity of ZnO and TiO₂ to *Escherichia coli* cells, *J. Scientific report*, vol. 6:35243(2016), 1–13.

[36]. F.Z. Haque, N. Singh, P. Pandey, M.R. Parra, study of zinc oxide nano/micro rods on ITO and glass substrates, *Optik* 124(20), 2013, 4167–4171.

[37]. H. Jung, D.B. Kim, B. Gweon, S.Y. Moon, W. Choe, Enhanced inactivation of bacterial spores by atmospheric pressure plasma with catalyst TiO₂, *J. Appl. Catal. B* 93(2010) 212–216.

[38]. C.-C. Lin, Y.-Y. Li, Synthesis of ZnO nanowires by thermal decomposition of zinc acetate dihydrate, *J. Mater. Chem. Phys.* 113 (2009) 334–337